BRIEF COMMUNICATION
PUBLISHED ONLINE: 19 SEPTEMBER 2016 | DOI: 10.1038/NCHEMBIO.2176
nature chemical biology

Compounds that select against the tetracycline-resistance efflux pump

Laura K Stone[1], Michael Baym[1], Tami D Lieberman[1], Remy Chait[1,2], Jon Clardy[3] & Roy Kishony[1,4]*

We developed a competition-based screening strategy to identify compounds that invert the selective advantage of antibiotic resistance. Using our assay, we screened over 19,000 compounds for the ability to select against the TetA tetracycline-resistance efflux pump in *Escherichia coli* and identified two hits, β-thujaplicin and disulfiram. Treating a tetracycline-resistant population with β-thujaplicin selects for loss of the resistance gene, enabling an effective second-phase treatment with doxycycline.

The use of antibiotics promotes the emergence and spread of resistant strains, which raises public health concerns[1]. Since the cost of resistance is typically small[2,3], resistance alleles often remain in the population after fixation, even in the absence of antibiotics[2]. Therefore, inverting the evolutionary advantage of resistant bacteria and driving them back to drug susceptibility requires treatments that impose substantial fitness costs to resistance alleles[4–7].

Collateral sensitivity, which occurs when an allele that confers resistance to one drug simultaneously increases sensitivity to another drug[9], can be used to select against resistant strains in favor of drug susceptibility[8]. In such cases, bacteria that have evolved resistance to drug A can be penalized by their increased sensitivity to drug B. Treatment with drug B can then drive the population back to drug-A susceptibility[8]. In studies on collateral sensitivity, many drugs have been found that select against *de novo* resistance mutations[8–15]. However, only a few drugs are known to select against specialized resistance genes and cassettes[16–18] that encode major modes of clinical resistance, such as efflux pumps, drug degrading enzymes, or modified targets[19], and systematic screens for such selection-inverting compounds have been limited[20].

Focusing on tetracycline resistance, we designed a high-throughput screen to identify selection-inverting compounds, small molecules that confer a disadvantage to a resistant strain compared to its susceptible parent. Tetracycline is a broad-spectrum antibiotic whose use has dwindled in part because of widespread resistance[21]. The TetA efflux pump, often carried by transposons, is one of the most prevalent tetracycline-resistance mechanisms[21]. In our assay, equally fit tetracycline-susceptible (Tet^S) and -resistant (Tet^R, containing TetA) strains are differentially labeled with fluorescent proteins and competed on diffusion-generated gradients of test compounds[20] (**Fig. 1a**). This competition may be altered by a compound that preferentially inhibits one of the strains (**Fig. 1b**). For control compounds, we used doxycycline, a tetracycline analog that selects for tetracycline resistance (**Fig. 1c**); fusaric acid, a known molecule that selects against the TetA efflux pump but is of limited utility because of its toxicity[16,22] (**Fig. 1d**); ciprofloxacin, an antibiotic eliciting no or very mild selection for tetracycline resistance (**Supplementary Results**, **Supplementary Fig. 1a**); and a DMSO vehicle control (**Supplementary Figs. 1b** and **2**). The medium was supplemented with anhydrous tetracycline (ATC) at concentrations that induce expression of TetA but have no detectable effects on growth. We developed custom 48-well plates and an imaging platform for high-throughput automation of the assay (**Supplementary Figs. 1b** and **3**, see Online Methods).

Screening 19,769 compounds, we identified two that can select against the tetracycline-resistance efflux pump. The primary screen identified 38 hits from three libraries: 30 known bioactives (0.34% of 8,752 screened), 8 natural-product extracts (0.12% of 6,441), and 0 commercial library compounds (of 4,576, **Supplementary Table 1**). We verified positive hits by retesting them in our assay, in duplicate, with a dye swap to control for autofluorescence. Of our initial 38 hits, two hits from the bioactives collection retested positive in both replicates: disulfiram and β-thujaplicin (also known as hinokitiol, **Fig. 1d** and **Supplementary Fig. 4**). Disulfiram is an FDA-approved drug (Antabuse) for treating alcoholism, and it acts synergistically with tetracycline in susceptible strains[23]. β-Thujaplicin has widespread antifungal and antibacterial activity[24]. While these compounds were already known to have antibacterial activity[24,25], their ability to select against tetracycline resistance is a newly discovered property.

We evaluated the potency and selectivity of these compounds by testing them on the resistant and susceptible strains, separately and in competition. Measuring the dose–responses of disulfiram, β-thujaplicin, and the fusaric acid control alone in liquid medium further confirmed their differential ability to inhibit the growth of Tet^R compared to Tet^S strains (**Supplementary Fig. 5**; half-maximal inhibitory concentration (IC_{50}) of Tet^R, Tet^S; disulfiram: $91 \pm 3\,\mu M$, $133 \pm 4\,\mu M$, $P < 10^{-5}$; β-thujaplicin: $30 \pm 1\,\mu M$, $39 \pm 4\,\mu M$, $P < 10^{-3}$; fusaric acid: $106 \pm 6\,\mu M$, $133 \pm 14\,\mu M$, $P = 10^{-3}$; mean ± s. d., $n = 6$, Student's t-test). We define potency as the IC_{50} against the sensitive strain. To determine selectivity, we performed a competition assay in liquid medium, mixing fluorescently labeled Tet^S and Tet^R strains 1:1, growing them in a linear dilution series of each compound for 24 h, and using flow cytometry to measure their final ratio (N^S/N^R, **Supplementary Fig. 6a**). Disulfiram and β-thujaplicin, as well as the fusaric acid control, gave a competitive advantage to the Tet^S over the Tet^R strain (**Fig. 2a**,**b** and **Supplementary Fig. 6b–e**). For each compound, we then defined selectivity as the average selection (average of $\log_{10}(N^S/N^R)$ over the range where at least one of the strains can grow, **Supplementary Fig. 6c–e**). We decided to focus on β-thujaplicin because of its better potency and superior selectivity and the availability of chemical analogs. A kill-curve assay applying β-thujaplicin to co-cultures of fluorescently labeled Tet^S and Tet^R strains showed specific killing of the Tet^R over the Tet^S strain (>3-fold difference in the bactericidal concentration; **Supplementary Fig. 7**).

To understand which chemical moieties of β-thujaplicin are critical for its antibacterial and selection properties, we measured the potency and selectivity of various β-thujaplicin analogs (**Fig. 2a**,**b**; **Supplementary Figs. 5**, **6**, **8** and **9**; **Supplementary Tables 2** and **3**). β-Thujaplicin far exceeded its analogs in both potency and selectivity (**Fig. 2b**). The regioisomer, α-thujaplicin, had the same potency, but showed no selection between the Tet^S and Tet^R strains (**Fig. 2b**,

[1]Department of Systems Biology, Harvard Medical School, Boston, Massachusetts, USA. [2]Institute of Science and Technology–Austria, Maria Gugging 3400, Klosterneuburg, Austria. [3]Department of Biological Chemistry and Molecular Pharmacology, Harvard Medical School, Boston, Massachusetts, USA. [4]Department of Biology and Department of Computer Science, Technion–Israel Institute of Technology, Haifa, Israel. *e-mail: rkishony@technion.ac.il

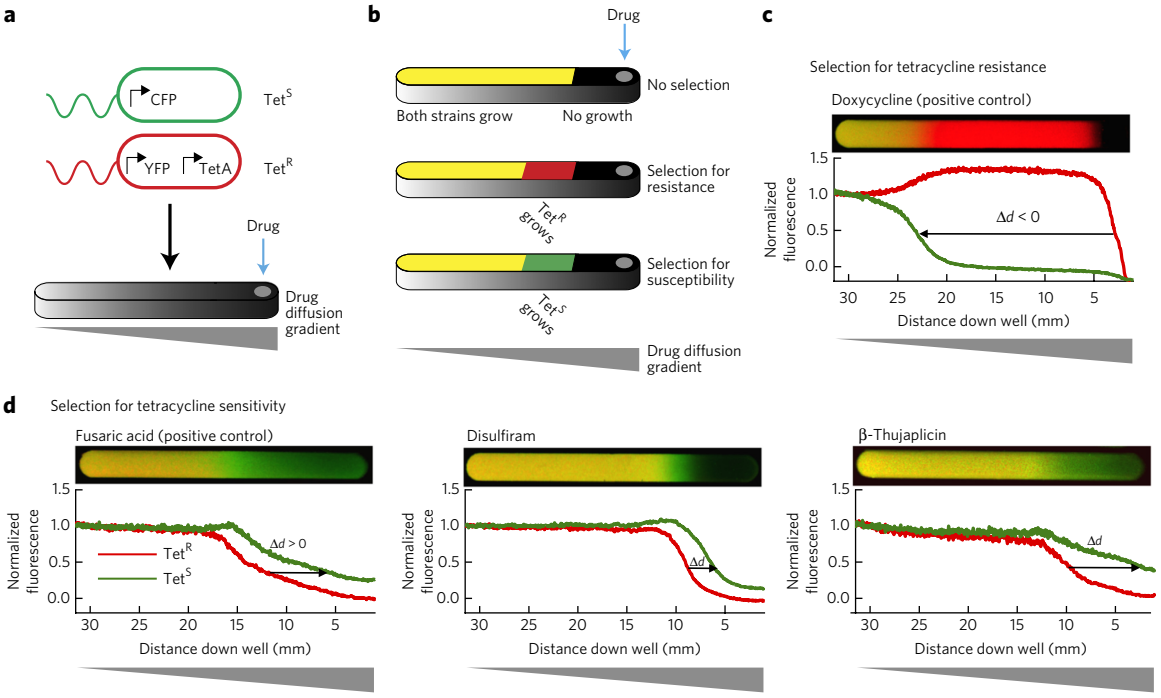

Figure 1 | A high-throughput diffusion-based screen identifies compounds that select against tetracycline resistance. (**a**) Tetracycline-susceptible (Tet^S; CFP, shown in green) and tetracycline-resistant strains (Tet^R; TetA, YFP, shown in red; a dye-swap control is also used) are mixed 1:1 and plated on agar lanes with diffusion gradients of locally spotted drugs. (**b**) Fluorescence imaging reveals regions of selection along the drug gradient. Areas where both strains can grow maintain a 1:1 ratio and appear yellow; areas where neither strain can grow appear dark, whereas areas selecting for resistance or susceptibility appear red or green, respectively. (**c**,**d**) Automated image analysis identifies the distance from the drug spot where each strain can grow (defined by half-maximal fluorescence). The difference between these points (Δd) is used to score hits: $\Delta d < 0$ indicates selection for resistance (**c**, doxycycline control), and $\Delta d > 0$ indicates selection against resistance (**d**, fusaric acid control). Hit compounds disulfiram and β-thujaplicin select for tetracycline susceptibility (**d**).

compound **1**; **Supplementary Figs. 5d** and **6f** and **Supplementary Table 2**). From this structure–activity relationship, we infer that the hydroxyl group is required for potency, while the presence and position of the isopropyl group affects the degree of selection (**Fig. 2b**).

While the hit compounds we identified preferentially inhibit the Tet^R strain, it remained unclear whether this cost of resistance was sufficient to evolve a resistant population back to tetracycline susceptibility. To assess this, we propagated eight replicate populations of the Tet^R strain in β-thujaplicin gradients for 7 d (each day propagating the population from the highest drug concentration that shows growth). In all eight populations, the frequency of tetracycline-resistant cells rapidly decreased, quickly falling below detection levels (10^{-6}, **Fig. 2c** and **Supplementary Fig. 10**). To see if these populations, now tetracycline sensitive, would become tetracycline resistant upon treatment with doxycycline, we next passaged them in doxycycline gradients for 3 d. Only one of the eight populations regained tetracycline resistance. All other cultures permanently lost tetracycline resistance upon β-thujaplicin treatment through deletion of *tetA* (**Supplementary Fig. 11**; Sanger sequencing revealed no mutations in *marR*, the repressor of the multiple-antibiotic-resistance operon), enabling effective doxycyline treatment. This observation suggests a two-phase treatment protocol in which a selection-inverting compound converts a resistant population to susceptibility and a traditional antibiotic clears any remaining bacteria.

To understand the frequency of tetracycline-resistance loss and its underlying genotypic mechanisms, we performed a second selection experiment, isolating β-thujaplicin-resistant (122 μM minimum inhibitory concentration (MIC)) mutants derived from the Tet^R strain (91 μM MIC) and assayed their doxycycline phenotype. These mutants had the same β-thujaplicin MIC as the Tet^S strain (122 μM); no colonies appeared at or above this concentration. The vast majority of these isolates became doxycycline susceptible (Tet^S) upon β-thujaplicin selection (98 of 99, **Fig. 2d**). PCR amplification of the *tetA* gene showed that most had *tetA* deleted (77 of 99), while the rest had a 0.5–1 kb insertion in *tetA* (21 of 99, **Fig. 2d** and **Supplementary Fig. 12**). Whole-genome sequencing of six *ΔtetA* isolates and four isolates with insertions in *tetA* confirmed these changes. Two *ΔtetA* isolates also had single nucleotide polymorphisms (SNPs), one in the glutathione/cysteine ABC transporter gene *cydD* and one upstream of the tyrosine transporter gene *tyrP*, but neither of these isolates displayed higher levels of β-thujaplicin resistance (**Supplementary Table 4**). The one isolate that became β-thujaplicin resistant without losing *tetA* had a frameshift mutation in $marR^{26}$ (**Supplementary Table 4**), suggesting a possible rare mechanism to evolve β-thujaplicin resistance without losing the tetracycline efflux pump. While this mutant had the same β-thujaplicin MIC as other β-thujaplicin-resistant mutants, it also had a somewhat higher doxycycline MIC (234 μM) compared to the Tet^R strain (156 μM MIC), highlighting the threat of potential cross resistance. However, the *marR* mutant occurred at much lower frequencies (10^{-6}) compared to deletions or insertions in *tetA* (10^{-4}), consistent with previous studies on SNP-based resistance compared to transposon loss[18]. Together, these data show that the vast majority of β-thujaplicin resistance appears through null insertions in or deletions of the *tetA* gene, while only rare cases evolve resistance to β-thujaplicin through more general resistance pathways, without loss of tetracycline resistance. Similar results appear for disulfiram selection (78 of 81 lost tetracycline resistance: 75 Δ*tetA*, 1 frameshift deletion in *tetA*, 1 insertion in *tetA*, and 1 insertion in *tetR*, **Fig. 2d**; **Supplementary Figs. 13** and **14**).

Compounds that select against resistance genes can be systematically identified through competition-based screening and can be used in a two-phase treatment regimen against resistant infections. In this strategy, a first-phase treatment with a selection-inverting compound turns the resistant population sensitive, allowing an effective second-phase treatment with the classical antibiotic. The efficacy of this

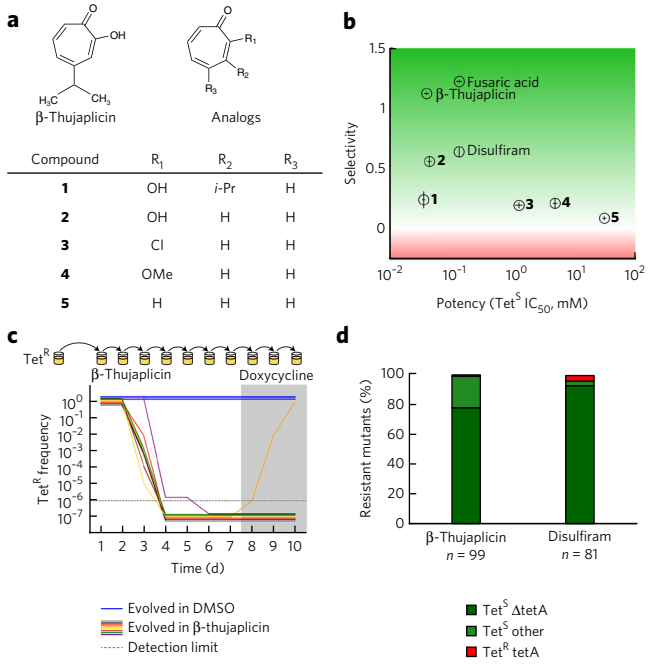

Figure 2 | β-Thujaplicin and disulfiram select for loss of tetracycline resistance. (**a**) β-Thujaplicin and its analogs. (**b**) The advantage of the Tet^S over the Tet^R strain at each drug concentration is measured by the ratio N^S/N^R, determined by flow cytometry and normalized to the ratio of N^S/N^R with no drug. The selectivity of the drug is represented by the average selection (normalized $\log_{10}(N^S/N^R)$) across the concentrations at which at least one of the strains can grow. Examining all compounds for selectivity (mean ± s.d., $n = 5$) and potency (Tet^S IC_{50}, mean ± s.d., $n = 6$) shows that β-thujaplicin exerts the greatest selection for Tet^S among its analogs and has better potency compared with fusaric acid. (**c**) When evolved in β-thujaplicin (days 1–7), eight parallel populations of the Tet^R strain lost their tetracycline-resistance phenotype, with the frequency of resistant cells rapidly falling below the detection limit (10^{-6}). In a second selection phase (days 8–10), the lineages were evolved in doxycycline, yet the majority did not regain tetracycline resistance (7 of 8). In contrast, all (3 of 3) lineages that were evolved for 7 d in DMSO (blue) remained tetracycline resistant. Points are offset slightly to resolve overlaps. (**d**) The vast majority of β-thujaplicin- and disulfiram-resistant mutants selected from the Tet^R strain lost phenotypic resistance to tetracycline (Tet^S, green and light green). Most tetracycline-susceptible (Tet^S) mutants completely lost *tetA* (green); others (light green) had insertions within *tetA* (21 of 99 β-thujaplicin mutants, 1 disulfiram mutant) or *tetR* (1 disulfiram mutant) or had an 11-bp deletion within *tetA* (1 disulfiram mutant). Only 1 β-thujaplicin-resistant mutant and 3 disulfiram-resistant mutants remained tetracycline resistant (Tet^R, red) with an intact *tetA* gene.

approach is enhanced by the presence of many antibiotic resistance genes on mobile elements[21,26,27], which can be spontaneously lost at high frequencies[16,27]. This strategy can be adapted to other organisms and resistance mechanisms for counter selection in synthetic biology, microbial evolution, agriculture, and possibly therapeutics. However, bacterial populations can escape this treatment regimen through cross resistance mutations (such as the *marR* mutant) or mutations that provide resistance to the selection-inverting compound without losing antibiotic resistance. Resistance to the antibiotic in the second phase could further arise as a result of incomplete fixation of the antibiotic-sensitive mutations during the first phase or because of reversal of these mutations in the second phase of treatment. The clinical application of this strategy may further be precluded by its extended treatment times. Despite these difficulties, we hope these findings will inspire future therapeutic paradigms that can reverse the evolution of resistance[4]. Two-phase treatments beginning with selection-inverting compounds that counteract the evolutionary advantage of resistance could add valuable tools to our antimicrobial arsenal.

Received 4 November 2015; accepted 14 July 2016; published online 19 September 2016

Methods

Methods and any associated references are available in the online version of the paper.

Accession codes. The sequences reported in this article have been deposited in the National Center for Biotechnology Information Sequence Read Archive database (accession number SRP073071).

References

1. World Health Organization. *Antimicrobial Resistance: Global Report on Surveillance* (World Health Organization, 2014).
2. Andersson, D.I. & Hughes, D. *Nat. Rev. Microbiol.* **8**, 260–271 (2010).
3. Lenski, R.E., Simpson, S.C. & Nguyen, T.T. *J. Bacteriol.* **176**, 3140–3147 (1994).
4. Baym, M., Stone, L.K. & Kishony, R. *Science* **351**, aad3292 (2016).
5. Chait, R., Craney, A. & Kishony, R. *Nature* **446**, 668–671 (2007).
6. Palmer, A.C., Angelino, E. & Kishony, R. *Nat. Chem. Biol.* **6**, 105–107 (2010).
7. Chait, R., Palmer, A.C., Yelin, I. & Kishony, R. *Nat. Commun.* **7**, 10333 (2016).
8. Imamovic, L. & Sommer, M.O.A. *Sci. Transl. Med.* **5**, 204ra132 (2013).
9. Szybalski, W. & Bryson, V. *J. Bacteriol.* **64**, 489–499 (1952).
10. Lázár, V. *et al. Mol. Syst. Biol.* **9**, 700 (2013).
11. Hiramatsu, K. *et al. Int. J. Antimicrob. Agents* **39**, 478–485 (2012).
12. Chao, L. *Nature* **271**, 385–386 (1978).
13. Lukens, A.K. *et al. Proc. Natl. Acad. Sci. USA* **111**, 799–804 (2014).
14. Gonzales, P.R. *et al. Nat. Chem. Biol.* **11**, 855–861 (2015).
15. Kim, S., Lieberman, T.D. & Kishony, R. *Proc. Natl. Acad. Sci. USA* **111**, 14494–14499 (2014).
16. Bochner, B.R., Huang, H.C., Schieven, G.L. & Ames, B.N. *J. Bacteriol.* **143**, 926–933 (1980).
17. Merlin, T.L., Davis, G.E., Anderson, W.L., Moyzis, R.K. & Griffith, J.K. *Antimicrob. Agents Chemother.* **33**, 1549–1552 (1989).
18. Stone, G.W. *et al. Antimicrob. Agents Chemother.* **48**, 477–483 (2004).
19. Wright, G.D. *Chem. Commun.* **47**, 4055–4061 (2011).
20. Chait, R., Shrestha, S., Shah, A.K., Michel, J.-B. & Kishony, R. *PLoS One* **5**, e15179 (2010).
21. Chopra, I. & Roberts, M. *Microbiol. Mol. Biol. Rev.* **65**, 232–260 (2001).
22. Wang, H. & Ng, T.B. *Life Sci.* **65**, 849–856 (1999).
23. Ejim, L. *et al. Nat. Chem. Biol.* **7**, 348–350 (2011).
24. Anderson, A.B. & Gripenberg, J. *Acta Chem. Scand.* **2**, 644–650 (1948).
25. Phillips, M., Malloy, G., Nedunchezian, D., Lukrec, A. & Howard, R.G. *Antimicrob. Agents Chemother.* **35**, 785–787 (1991).
26. Alekshun, M.N. & Levy, S.B. *Cell* **128**, 1037–1050 (2007).
27. Katayama, Y., Ito, T. & Hiramatsu, K. *Antimicrob. Agents Chemother.* **44**, 1549–1555 (2000).

Acknowledgments

We thank D. Rudner, R. Mazitschek, and R. Moellering for helpful insights; J. Horn and J. Marchionna for custom screening plate manufacture and technical advice; D. Flood and S. Rudnicki for technical support in the primary screen; and J. Wang and J. Moore for technical support in the flow cytometry assay. All primary screening was performed at Harvard Medical School ICCB-L Screening Facility. This work was supported in part by National Institute of Allergy and Infectious Diseases grant U54 AI057159, US National Institutes of Health grants R01 GM081617 (to R.K.) and GM086258 (to J.C.), European Research Council FP7 ERC grant 281891 (to R.K.) and a National Science Foundation Graduate Fellowship (to L.K.S.).

Author contributions

L.K.S., J.C., and R.K. designed research; L.K.S. performed experiments and analyzed data; M.B. and R.C. built the imaging setup and M.B. developed the automation; L.K.S. and M.B. performed genomic sequencing; T.D.L. analyzed genomic sequencing data; R.C. contributed the initial plate and assay design; L.K.S. and R.K. wrote the manuscript.

Competing financial interests

The authors declare no competing financial interests.

Additional information

Any supplementary information, chemical compound information and source data are available in the online version of the paper. Reprints and permissions information is available online at http://www.nature.com/reprints/index.html. Correspondence and requests for materials should be addressed to R.K.

ONLINE METHODS

Strains and media. All experiments were conducted in low-salt LB medium (RPI, catalog no. L24065), supplemented with bacto agar (BD Falcon) when noted. Drug solutions were made from powder stocks (anhydrotetracycline hydrochloride (ATC), catalog no. 37919 (Sigma, analytical standard); doxycycline hyclate, catalog no. D9891 (Sigma, ≥98.0%); ciprofloxacin, catalog no. 17850 (Fluka, ≥98.0%); fusaric acid, catalog no. AC19896 (Fisher, 99%); β-thujaplicin, catalog no. 469521 (Sigma, 99%); disulfiram, catalog no. 86720 (Sigma, ≥97.0%); α-thujaplicin (**Fig. 2b**, compound **1**), catalog no. 088-08701, (Wako, ≥98.0%); tropolone (compound **2**), catalog no. T89702 (Sigma, 98%); 2-chloro-2,4,6-cycloheptatrien-1-one (compound **3**, chlorotropone), catalog no. 669571, (Sigma, ≥98.0%); 2-methoxy-2,4,6-cycloheptatrien-1-one (compound **4**, methoxytropone), catalog no. 137-15711 (Wako, ≥98.0%); tropone (compound **5**), catalog no. 252832 (Sigma, 97%) and filter-sterilized. All drug stocks were dissolved in DMSO at 15 mg/mL, except anhydrotetracycline hydrochloride, which was dissolved in EtOH at 1 mg/mL.

Strain construction and designations are in **Supplementary Table 5**. Plasmids expressing YFP or CFP under the P_R promoter[28] were constructed from the pZ vector system[29]. Assay strains were grown from single colonies to saturation in low-salt LB. Cell concentrations were measured by optical density at 600 nm (OD_{600}) and plate count. Aliquots were stored in 15% glycerol at 80 °C. Fresh aliquots were used for each experiment.

Custom assay plate. We tailored a design for 48-well plates composed of 2 rows of 24 lanes[20] to be compatible with high-throughput screening robots by lowering the plate's skirt and adding spacing bars so that air could escape as the agar cools while the plates were stacked (**Supplementary Fig. 3**).

Screen for selection inverters. Custom 48-well screening plates were filled with 352 µL/well low-salt LB 1.5% bacto agar containing 80 ng/mL ATC using a Wellmate Stacker (Thermo Scientific). Approximately 1 µL/well test compounds were pinned onto the top of each lane using AFIX384FP6 (V&P Scientific) with FP6S pins (V&P Scientific) in rows A and I by the Seiko robot. Approximately 1 µL/well control compounds were pinned onto the top of each lane by hand using AFIX384FP (V&P Scientific) with FP6S pins (V&P Scientific) in appropriate wells. Each screening plate had at least one of each control: 15 mg/mL doxycycline, 15 mg/mL fusaric acid, 15 mg/mL ciprofloxacin, and DMSO vehicle control. Plates were stored at 4 °C for 24 h to allow the compounds to diffuse, creating concentration gradients down the length of the wells. Plates were then inoculated using a Wellmate Stacker with 112 µL/well frozen-cell aliquots diluted 1:100 in low-salt LB, 0.75% bacto agar containing 80 ng/mL ATC. Each test compound was tested twice, with the fluorescent markers switched between the tetracycline-susceptible and -resistant strains to identify autofluorescent compounds. One replicate was inoculated with a 1:1 ratio of pY:t17pC and the other was inoculated with a 1:1 ratio of pC:t17pY. Plates were incubated at 30 °C and 70% humidity for 16–18 h. Finally, plates were automatically imaged in three channels, brightfield, CFP (436/20 ex, 480/40 em), and YFP (500/20 ex, 530/20 em), with a Canon T3i using a custom-built robotic fluorescence imaging 'Macroscope' device[20].

As seen in **Figure 1**, the selection against resistance is concentration dependent—too much compound will kill both strains, while too little will allow both strains to grow. When screening for novel compounds that select against resistance, the concentration range in which they select is unknown. Employing diffusion gradients on agar allows rapid assessment of a continuous range of concentrations using small amounts of library compounds. Allowing the compounds to diffuse for 24 h permits the compound gradient to somewhat stabilize before adding bacteria (the diffusion rate decreases with time as the compounds equilibrate), thus somewhat decoupling compound diffusion and bacterial growth. Because the diffusion constants of most library compounds are unknown, their active range of concentration must be determined in follow-up studies using a defined dilution series of drug.

Screen analysis. The images were processed using a custom MATLAB script. The blue channel from the CFP image and the green channel from the YFP image were reduced to grayscale images. A shading correction is employed to address nonuniformity in the field of illumination. The images were further processed by subtracting the background (the median intensity of an area of no bacterial growth) and normalizing to an area of neutral selection (the median intensity of the DMSO controls). Next, an RGB overlay image was created with the susceptible strain image in the green channel and the resistant strain image in the red channel, regardless of the fluorescent proteins involved. Using this overlay, the pixel-intensity data was isolated for each well and the median was taken across the width of the well for the red and green channels. Wells with no inhibition of either strain were filtered out using a minimum intensity threshold. The remaining wells were scored by subtracting the distance to the half-maximum growth of the resistant strain from the distance to the half-maximum growth of the susceptible strain down the length of the well (Δd). Overlay images were evaluated by eye in addition to the automated ranking of hits. Using the Δd metric, doxycycline (selection for resistance control) and fusaric acid (selection against resistance control) were identified in comparison to ciprofloxacin (inhibition with no selection control) and DMSO (no inhibition or selection control). The Z' factor was 0.62 for the fusaric acid control and 0.87 for the doxycycline control.

Growth curve assay. Clear, flat-bottomed 96-well plates (Corning 3370) were filled with 150 µL/well low-salt LB with 80 ng/mL ATC containing linear dilution series of DMSO and ~10^4 cells/well WT (Tet^S) or ~10^4 cells/well t17 (Tet^R) cells. Experiments were run in parallel with four replicates. The plates were incubated for 24 h at 30 °C, 70% humidity with shaking. Growth was measured every 12 min by OD_{600} on an Envision plate reader (PerkinElmer).

Petri competition assay. Petri dishes (100 mm × 15 mm, BD Falcon) were filled with 20 mL low-salt LB 1.5% bactoagar containing 80 ng/mL ATC. Drug stocks were pipetted onto the plate (3 µL of 15 mg/mL fusaric acid, 1 µL of 15 mg/mL β-thujaplicin, and 6 µL of 15 mg/mL disulfiram dissolved in DMSO) and allowed to diffuse at 4 °C for 24 h. The plates were then inoculated with 100 µL of a 1:100 dilution of frozen-cell aliquots in PBS. One replicate is inoculated with a 1:1 ratio of pY:t17pC and the other is inoculated with a 1:1 ratio of pC:t17pY. Plates were incubated at 30 °C and 70% humidity for 16–18 h, then imaged in brightfield, CFP, and YFP with the 'Macroscope' device[20].

Kill curve assay. Frozen aliquots of fluorescently labeled Tet^R and Tet^S cells (pY, t17pC, pC, and t17pY) were diluted 1:10^4 in 20 mL LB with 80 ng/mL ATC and grown to ~0.05 OD_{600} at 30 °C, 250 r.p.m. Tet^S and Tet^R were then mixed 1:1 according to OD_{600} measurement (two dye swaps, pY:t17pC and pC:t17pY). A tenfold dilution series of these initial cell mixtures (t = 0) was plated onto LB–agar petri dishes to count initial colony-forming units (CFU). These two co-cultures were then aliquoted 1 mL/well into a row of a 96-deep-well plate and β-thujaplicin was added to each well at a series of concentrations (indicated in **Supplementary Fig. 6**). To measure surviving cells as a function of time, 50 µL aliquots were taken at 10, 20, 30, 45, 60, 90 and 180 min time points and an 8-step, tenfold dilution series of each well at each time point was drop-plated (7 µL/drop) onto an omnitray filled with 30 mL LB–agar to count CFU (total of 2 dye swaps × 12 drug concentrations × 7 time points × 8 dilutions = 1,344 drops plated for CFU). Plates were incubated at 30 °C for ~12 h. Colonies were imaged in brightfield, CFP, and YFP with the 'Macroscope' device[20] and counted using MATLAB scripts and visual inspection. CFU/mL of each strain was calculated based on the most dilute drop with ≥10 colonies of that strain at each drug concentration, at each time point.

IC_{50} measurements. Clear, flat-bottomed 96-well plates (Corning 3370) were filled with 150 µL/well low-salt LB containing linear dilution series of drug, ~10^4 cells/well WT (Tet^S), and ~10^4 cells/well t17 (Tet^R) cells. Experiments were run in parallel: six replicates with and six replicates without 80 ng/mL ATC show that fitness differences are dependent on the expression of the TetA pump. The plates were sealed with Aeraseal (Excel Scientific) to limit evaporation and incubated for 24 h at 30 °C with shaking at 900 r.p.m. on Titramax 1000 (Heidolph). Growth was measured by OD_{600} on a Victor3 plate reader (PerkinElmer). The dose–responses are fit to a 4-parameter logistic function $c + (d–c)/(1 + (x/a)^b)$, where a is the IC_{50}, b is the slope parameter, c is the minimum response level, and d is the maximum response level. Normality

and homogeneity of variance confirmed by Shapiro-Wilk test and Levene's test, respectively. Significance was determined by Student's *t*-test.

Flow cytometry competition assay. Clear, flat-bottomed 96-well plates (Corning 3370) were filled with 150 µL/well low-salt LB containing linear dilution series of drug and ~10^4 cells/well fluorescently labeled Tet^S and ~10^4 cells/well fluorescently labeled Tet^R cells. Experiments were run in parallel with a dye swap (pY & t17pC in one set of plates and pC & t17pY in another set) to show that fitness differences do not depend on the fluorescent proteins and with and without 80 ng/mL ATC to show that fitness differences are dependent on the expression of the TetA pump. The plates were sealed with Aeraseal (Excel) to limit evaporation and incubated for 24 h at 30 °C with shaking at 900 r.p.m. on Titramax 1000 (Heidolph). The saturated cultures were diluted 1:100 by pinning ~1.5 µL/well culture into 150 µL PBS with VP407 (V&P Scientific). Cells were counted by flow cytometry (Becton Dickinson LSRII; CFP excited at 405 nm, emission detected through 505LP and 525/550 nm filters; YFP excited at 488 nm, emission also detected through 505LP and 525/550 nm filters). The ratio of Tet^S to Tet^R cells (N^S/N^R) was normalized to the mean N^S/N^R of eight no-drug wells on each plate. Results in **Figure 2b** are the average of five replicates performed with pC and t17pY cells and 80 ng/mL ATC.

Passaging experiment. Clear, flat-bottomed 96-well plates (Corning 3370) were filled to a final volume of 150 µL/well low-salt LB with 80 ng/mL ATC. Each column contained a linear dilution series of β-thujaplicin or doxycycline. Each plate included one column inoculated with WT ancestral control, one column inoculated with t17 ancestral control, and one column with no bacteria to control for contamination. Nine columns contained replicate populations of t17 passaged each day into fresh β-thujaplicin for 7 d, then in doxycycline for 3 d (β-thujaplicin evolved strains). In addition, 3 replicate populations of t17 were passaged in a fixed DMSO concentration equivalent to the highest DMSO concentration used in the β-thujaplicin dilution series (DMSO evolved strains). Plates were inoculated with ~10^4 cells/well. The plates are sealed with Aeraseal (Excel) to limit evaporation and incubated for 22 h at 30 °C with shaking at 900 r.p.m. on Titramax 1000 (Heidolph). Growth was measured by OD_{600} on a Victor3 plate reader (PerkinElmer). For each evolved strain, the well containing the highest drug concentration with $OD_{600} \geq 0.4$ was diluted and propagated daily into fresh drug plates with ~10^4 cells/well. The remainder of the well was stored in 15% glycerol at 80 °C. The wells with WT and t17 ancestral controls and no drug were also stored in 15% glycerol at 80 °C to serve as controls for later follow up. One of the nine β-thujaplicin lineages was contaminated in storage and is excluded from **Figure 2c**.

The Tet^R frequency was measured by creating a tenfold dilution series of stored evolved strains and ancestral controls in PBS. Using VP407, ~1.5 µL/well of these dilution series and the storage wells were pinned onto one non-treated omnitray (Thermo Scientific) containing 30 mL low-salt LB 1.5% bactoagar and one non-treated omnitray containing 30 mL low-salt LB 1.5% bactoagar and 20 µg/mL doxycycline. The plates were incubated at 30 °C for 22 h and then imaged. Growth was then measured by eye with positive growth being that at least one colony grew from the spot. The CFU/mL of the dilution series was calibrated by plating 50 µL of select wells onto petri dishes containing 20 mL low-salt LB 1.5% bacto agar. The data from pinning is precise to one order of magnitude. The accuracy of this method was confirmed by plating 50 µL/well of a subset of samples onto petri dishes containing 20 mL low-salt LB 1.5% bactoagar and onto petri dishes containing 20 mL low-salt LB 1.5% bacto agar and 20 µg/mL doxycycline.

Resistant mutant selection. The t17 strain was streaked on a low-salt LB 1.5% bacto agar petri dish and grown overnight at 30 °C. A single colony was picked and grown overnight in low-salt LB to saturation (~2×10^9 cells/mL). This culture was spun down at 3,000 r.p.m. at 4 °C and the supernatants decanted. The culture was resuspended in PBS, spun down again, the supernatants decanted, and resuspended in PBS to a density of ~10^7 cells/mL. Petri dishes containing 20 mL low-salt LB 1.5% bacto agar, 80 ng/mL ATC, and either 40 µg/mL disulfiram or 15 µg/mL β-thujaplicin were inoculated with ~10^6 t17 cells/plate. The plates were incubated at 30 °C, 70% humidity, protected from light. Disulfiram plates were incubated for 3 d and β-thujaplicin plates were incubated for 6 d.

One hundred colonies from the β-thujaplicin and disulfiram selection plates were streaked onto LB agar petri dishes and incubated overnight at 30 °C. One colony from each streak was transferred to deep 96-well plates containing 1 mL/well low-salt LB. A subset of the plate was inoculated with WT or t17 ancestral controls or left empty to control for cross contamination. The plates were sealed with Aeraseals and incubated at 30 °C with 600 r.p.m. shaking on a Titramax. Using VP407, ~1.5 µL/well was transferred from these overnight plates onto omnitrays containing low-salt LB 1.5% bactoagar, 80 ng/mL ATC, and drug (5, 10, 15, 20, 25, 30 µg/mL β-thujaplicin; 10, 20, 30, 40, 50, 60 µg/mL disulfiram; 0, 0.1, 1, 5, 10, 20, 40, 60, 80, 100 µg/mL doxycycline). Omnitrays were incubated at 30 °C for 20 h. Plates were imaged and growth was recorded (single colonies or films were recorded as no growth). The minimum inhibitory concentration (MIC) was determined as the lowest concentration at which the strains did not grow.

Detection of *tetA*, *tetR*, and *marR* by PCR. The *tetA*, *tetR*, and *marR* genes were amplified with the primers (**Supplementary Table 6**) in 25 µL reactions using 0.2 µL OneTaq (New England BioLabs) according to the supplier's protocol. Reactions were cycled 30 times, with an annealing temperature of 57 °C for *tetA* and *marR* and 59 °C for *tetR*. PCR product size was determined by gel electrophoresis on a 1% agarose gel (**Supplementary Figs. 9–11**). The bands were compared to a 1 kb DNA ladder (New England Biolabs) and their size was determined within 0.5 kb. The expected band size is 1,086 bp for *tetA*, 1,045 bp for *tetR*, and 611 bp for *marR* if the genes are present and uninterrupted. The *marR* PCR product was sent for Sanger sequencing (Genewiz, Boston, MA).

One mutant, disulfiram-resistant colony 19 (DsfRP1C10), was tetracycline susceptible despite having the expected length PCR products for both *tetA* and *tetR*. The *tetA* and *tetR* PCR products of this colony and the Tet^R t17 control were purified (QIAGEN) and Sanger sequenced at Genewiz, Boston, MA. Sanger sequencing revealed an 11 bp (frameshift) deletion in *tetA* in disulfiram-resistant colony 19 (DsfRP1C10).

Genomic sequencing of β-thujaplicin-resistant colonies. Genomic DNA was extracted from 1 mL cultures of eleven colonies and the ancestral t17 control using illustra bacteria genomicPrep Mini Spin Kit (GE Healthcare) following the supplier's protocol, except for eluting with water instead of elution buffer. Purified DNA was quantified using the Quant-iT High-Sensitivity DNA Assay Kit (Life Technologies). Sequencing libraries were prepared with the Nextera XT DNA Sample Preparation Kit (Illumina), using a previously described protocol[30]. Samples were sequenced using 100-bp paired-end reads on the HiSeq platform at Axeq Technologies, Seoul, South Korea. Adaptors were removed using cutadapt[31], reads were trimmed using Sickle, and trimmed reads were aligned to both the *E. coli* MC4100 reference genome and Tn10 (Genbank accession numbers NC_012759.1 and AF162223.1, respectively) using Bowtie2 (ref. 32). Over 99.7% of reads aligned to the reference genome, and average coverage across a sample ranged between 33× and 134× (median 65×). SNPs were identified using SAMtools[33] and consensus quality (FQ score) cutoff of less than 55 for inclusion. At each variant position that met this cutoff in at least one strain, a best call was made based on the aligned reads for each strain, and positions where all strains supported a variant were discarded. Small insertions and deletions (indels) were called using Dindel[34]. Candidate indels found in one strain were explicitly tested for in all strains; indels with at least 70% of reads in the region supporting the indel and at positions with an average of at least 10× coverage across isolates were accepted. Tn10 deletions were identified by the absence of reads aligning to the coding section of AF162223.1. Insertion elements were identified using RetroSeq[35] (FL score of 6 or 8).

28. Meyer, B.J., Maurer, R. & Ptashne, M. *J. Mol. Biol.* **139**, 163–194 (1980).
29. Lutz, R. & Bujard, H. *Nucleic Acids Res.* **25**, 1203–1210 (1997).
30. Baym, M. *et al. PLoS One* **10**, e0128036 (2015).
31. Martin, M. *EMBnet.Journal* **17**, 10–11 (2011).
32. Langmead, B. & Salzberg, S.L. *Nat. Meth.* **9**, 357–359 (2012).
33. Li, H. *et al. Bioinformatics* **25**, 2078–2079 (2009).
34. Albers, C.A. *et al. Genome Res.* **21**, 961–973 (2011).
35. Keane, T.M., Wong, K. & Adams, D.J. *Bioinformatics* **29**, 389–390 (2013).

doi:10.1038/nchembio.2176